Geomechanics and Engineering, *Vol. 29, No. 5 (2022) 487-496*
https://doi.org/10.12989/gae.2022.29.5.487

Reliability analysis of piles based on proof vertical static load test

Xiaole Dong[a], Xiaohui Tan*, Xin Lin[b], Xuejuan Zhang[c], Xiaoliang Hou[d] and Daoxiang Wu[e]

School of Resources and Environmental Engineering, Hefei University of Technology, Hefei 230009, China

(Received September 22, 2021, Revised April 12, 2022, Accepted April 26, 2022)

Abstract. Most of the pile's vertical static load tests in construction sites are the proof load tests, which is difficult to accurately estimate the ultimate bearing capacity and analyze the reliability of piles. Therefore, a reliability analysis method based on the proof load-settlement (*Q*-*s*) data is proposed in this study. In this proposed method, a simple ultimate limit state function based on the hyperbolic model is established, where the random variables of reliability analysis include the model factor of the ultimate bearing capacity and the fitting parameters of the hyperbolic model. The model factor $M = R_{uR} / R_{uP}$ is calculated based on the available destructive *Q*-*s* data, where the real value of the ultimate bearing capacity (R_{uR}) is obtained by the complete destructive *Q*-*s* data; the predicted value of the ultimate bearing capacity (R_{uP}) is obtained by the proof *Q*-*s* data, a part of the available destructive *Q*-*s* data, that before the predetermined load determined by the pile test report. The results demonstrate that the proposed method can easy and effectively perform the reliability analysis based on the proof *Q*-*s* data.

Keywords: model factor; pile; reliability analysis; ultimate bearing capacity; vertical static load test

1. Introduction

The various external conditions include the influence of construction of piles and inherent variability of soil cause uncertainties, which are unable to be fully reflected by a single factor of safety in the traditional allowable work design (AWD) for the bearing performance of piles. To better carry out the stability analysis and design of piles, it is necessary to perform reliability analysis of piles (Lee *et al*. 2009, Kim and Mission 2011).

In the reliability analysis of piles, an important task is to determine the ultimate bearing capacity (Khorrami and Derakhshani 2019). There are many methods to determine the statistical characteristics (e.g., the mean and the coefficient of variation (COV)) of the ultimate bearing capacity, such as the theoretical analysis method (Misra and Roberts 2009), the numerical simulation method (Fei *et al*. 2021), and the static load test method (Chinese Standard JGJ106-2014). For the first two methods, some simplified assumptions can lead to errors, such as the geometric dimensions of model (e.g., three-dimensional model is simplified to two-dimensional or one-dimensional model) and pile property (e.g., rigid, semi-rigid, and flexible). Moreover, same numerical methods and theoretical methods usually require strength and deformation parameters, which means that a large number of geotechnical experiments are unavoidable. Relatively, the static load test method is widely recognized as the most accurate of three methods for accessing the ultimate bearing capacity of piles, because it makes no assumptions and it can comprehensively reflect the influence of soil layers and the interaction between soil and pile.

In the static load tests, the *Q*-*s* data are important information for the reliability analysis of piles. Although the destructive test that the pile loaded to the damage is applied to accurately calculate the ultimate bearing capacity, such test is extremely rare due to the economic reasons. Therefore, most of the static load tests are proof tests, which the maximum load general is the predetermined load determined by the designers to be 1.5 times design load. Most of proof tests do not cause the damage of piles, so the ultimate bearing capacity obtained from the proof test are inaccurate. To solve the problem of insufficient number of *Q*-*s* data in a proof test, Luo *et al*. (2004) established a non-equal step length GM(1,1) model based on the gray system theory to predict the vertical ultimate bearing capacity of a single pile using the proof *Q*-*s* data, but this method needs to combine engineering experience to judge the shape of the *Q*-*s* curve, which is subjective and not conducive to statistical analysis of large amounts of data. Ching and Chen (2010) established a normalized *Q*-*s* curve full probability model for bored piles based on the Bayesian update theory. The *Q*-*s* curve is extrapolated to predict the settlement and ultimate bearing capacity at the high load level by using the *Q*-*s* data at the low load level. The theory of this method is complicated and is not friendly to engineers without comprehensive knowledge to calculate

*Corresponding author, Professor
E-mail: tanxh@hfut.edu.cn
[a]Ph.D. Student
E-mail: dongxiaole@mail.hfut.edu.cn
[b]B.D. Student
E-mail: linxin@mail.hfut.edu.cn
[c]B.D. Student
E-mail: 2020110714@mail.hfut.edu.cn
[d]Ph.D. Student
E-mail: xlhou@hfut.edu.cn
[e]B.D.
E-mail: wdx@hfut.edu.cn

ISSN: 2005-307X (Print), 2092-6219 (Online)

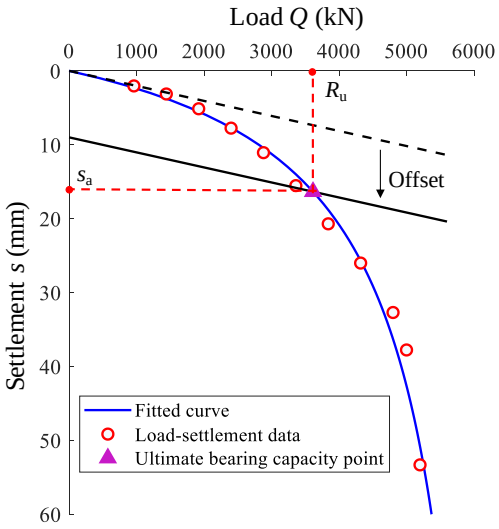

Fig. 1 Slope tangent method for estimating the ultimate bearing capacity

the reliability indices for a large number of proof *Q*-*s* data.

Therefore, this paper defines the model factor of ultimate bearing capacity by analyzing the correspondence between proof and destructive *Q*-*s* data based on a large amount of *Q*-*s* data collected from different construction sites and investigates the statistics characteristics of model factor. A simple ultimate limit state function is developed based on the hyperbolic model. An example for the reliability analysis of multiple sets of the proof tests is applied to illustrate the simplicity and efficiency of the proposed method.

2. Reliability analysis of piles

2.1 Ultimate bearing capacity of piles

By carrying out the static load test for a pile, a series of discrete values of load *Q* applied on the top of the pile and its corresponding settlement *s* are obtained. Then, the *Q*-*s* relationship can be fitted based on the discrete *Q*-*s* data using some analytical models, such as the hyperbolic model (Zhang *et al*. 2016) and the exponential model (Jia *et al*. 2018). In this study, the hyperbolic model is employed and is expressed as follows:

$$Q = \frac{s}{a + bs} \tag{1}$$

where Q is the vertical load applied on the top of a pile (unit: kN); s is the vertical settlement of the pile head (unit: mm); and a and b are fitting parameters of the hyperbolic model, whose units are mm/kN and 1/kN, respectively. A typical *Q*-*s* curve of the hyperbolic model is shown in Fig. 1, where the initial slope of the *Q*-*s* curve is $1/a$ and the maximum load is $1/b$.

After obtaining the analytical *Q*-*s* relationship of a pile, the ultimate bearing capacity can be estimated using various methods, such as the FHAW method (O'Neil and Reese 1990), the ISSMFE method (Selig and ISSMFE 1985), the Davisson method (Davisson 1972), and the slope tangent method (O'Rourke and Kulhawy 1985, Huffman *et al*. 2015). Among them, the FHAW method and the ISSMFE method are used to estimate the ultimate bearing capacity for a specified settlement and the analytical model; the Davisson method is used to estimate the ultimate bearing capacity according to the position of the cross-point of the *Q*-*s* curve and a straight line, where the slope of the straight line is a function of the Young's modulus and other material parameters; and the slope tangent method is a simplified updated version of the Davisson method. The slope tangent method is adopted in this paper to estimate the ultimate bearing capacity. As shown in Fig. 1, the main steps are as follows: (O'Rourke and Kulhawy 1985, Hirany and Kulhawy 2002, Ching and Chen 2010)

1) Perform curve fitting on the discrete *Q*-*s* data obtained from the static load test to get the *Q*-*s* curve and the fitting parameters a and b;

2) Draw a tangent line whose slope is $1/a$ at the origin of the *Q*-*s* curve in the *Q*-*s* coordinate system;

3) Use the tangent line as a reference, draw a parallel line with an offset of $B/120+4$ along the *s*-axis. Hence, the formula of the newly drawn line is

$$Q = \frac{1}{a}s + \frac{B}{120} + 4 \tag{2}$$

where B is pile diameter (unit: m).

4) Determine the ultimate bearing capacity R_u and the corresponding limit settlement s_a according to the intersection of the translational line and the *Q*-*s* curve. From Eq. (1), the corresponding relationship between R_u and s_a is obtained as

$$R_u = \frac{s_a}{a + b\,s_a} \tag{3}$$

2.2 Model factor of ultimate bearing capacity

For the destructive test of a pile, the force applied on the

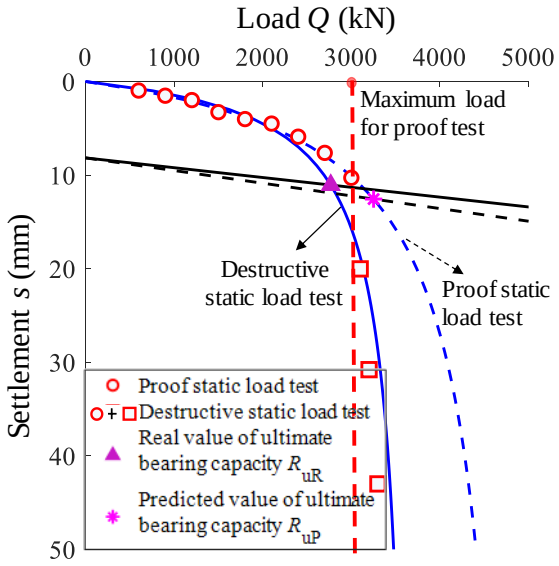

Fig. 2 Comparison of fitting curves of the *Q*-*s* data of destructive and proof load tests

top of a pile is gradually increased until plastic failure of the pile occurs. However, for the proof test of a pile, the force is only increased to the predetermined load which is usually smaller than the destructive load. Obviously, the proof *Q*-*s* data is regarded as a part of the destructive *Q*-*s* data. As shown in Fig. 2, the nine hollow circles represent the *Q*-*s* data obtained from the proof test, while the combination of the nine hollow circles and the three squares represents *Q*-*s* data obtained from the destructive test. Accordingly, the *Q*-*s* curve of the proof test (i.e., the dashed *Q*-*s* curve) is fitted based on the nine hollow circles, and the *Q*-*s* curve of the destructive test (i.e., the solid *Q*-*s* curve) is fitted based on all the twelve hollow data points. Because the settlement increases slowly with the load for the first nine data points, and then the settlement increases rapidly with the load for the last three points, the shapes of the *Q*-*s* curves of the destructive and proof tests are different, especially for the end parts of these two curves. Therefore, the ultimate bearing capacity estimated from the two *Q*-*s* curves are different.

The ultimate bearing capacities estimated by the destructive and the proof *Q*-*s* data are deemed as the real value of the ultimate bearing capacity (R_{uR}) and the predicted value of the ultimate bearing capacity (R_{uP}), respectively. As shown in Fig. 2, the horizontal coordinates of the solid triangle and the asterisk, which are estimated by the slope tangent method, represent the values of R_{uR} and R_{uP}, respectively.

By denoting a model factor M of the ultimate bearing capacity as the ratio of the real value to the predicted value of the ultimate bearing capacity using Eq. (4)

$$M = \frac{R_{uR}}{R_{uP}} \tag{4}$$

The advantage of the model factor M is dimensionless because R_{uR} and R_{uP} are obtained from the same pile and under the same geotechnical condition, so that it can weaken the influence of some factors (such as pile types, pile diameters, and soil properties) on estimating the ultimate bearing capacity. According to Eq. (4), the statistical characteristics of the real ultimate bearing capacity (R_{uR}) is estimated by the predicted ultimate bearing capacity (R_{uP}) and the model factor (M). The statistical characteristics of R_{uP} can be easily calculated because there are usually a large number of proof tests in a construction site. Thereby, a main effort is the estimation of the statistical characteristics of model factor (M), which is further described in Section '*3.2 Statistical analysis of model factor M*'.

2.3 Ultimate limit state function

The ultimate limit state function of a vertical loaded pile is generally expressed as the difference between the ultimate bearing capacity (R_{uR}) and load (Q)

$$Z = R_{uR} - Q \tag{5}$$

where Q is the vertical load applied to the top of the pile, which is estimated by the mean value of the predicted ultimate bearing capacity ($\mu(R_{uP})$) and the safety factor (F_s) using Eq. (6).

$$Q = \frac{\mu(R_{uP})}{F_s} \tag{6}$$

Substituting Eq. (4) into Eq. (5), Z is rewritten as

$$Z = MR_{uP} - Q \tag{7}$$

The R_{uP} in Eq. (7) is estimated by the slope tangent method. Therefore, Eq. (7) is further rewritten as follows

$$Z = \frac{Ms_a}{a + bs_a} - Q = \frac{Ms_a - Qa - Qbs_a}{a + bs_a} \tag{8}$$

Considering that the parameters a, b, and s_a are all positive values, which assures the denominator in Eq. (8) is

Table 1 Information of destructive static load tests

Site	Pile types	Number of piles N	Pile diameter (m)	Pile length (m)	Pile spacing (m)	Group piles' layout	Types of soil along the piles
D1	CBP	3	0.6	16	2.8	Square	Clay and silty clay
D2	CBP	5	0.6	13	2.8	Square	Clay and silty clay
D3	CBP	6	0.6	6	2.8	Square	Clay and silty clay
D4	CFG	3	0.5	23	2.0	Square	Silt, silty clay, and silty-fine sand
D5	CFG	3	0.4	22	1.4	Square	Silt, silty clay, and silty-fine sand
D6	CBP	3	1.0	21	8.0	Square	Silty clay, coarse sand, and weathered sandstone
D7	CBP	4	0.8	34	1.4	Square	Silty clay, clay, silt, and fine sand
D8	CBP	4	0.8	16	1.5	Square and triangle	Clay and silty clay
D9	CBP	6	0.8	43	18.0	Square	Silty clay, fine silt, and clay
D10	CBP	5	0.6	43	18.0	Square	Clay, silty clay, and fine silt

always non-negative, Eq. (8) is further simplified to: (Tan *et al*. 2017)

$$Z = Ms_{\mathrm{a}} - Qa - Qbs_{\mathrm{a}} \tag{9}$$

Eq. (9) will be used as the ultimate limit state function for the reliability analysis of piles in this study. As expressed in Eq. (4), the model factor M is the model uncertainty for the prediction of the ultimate bearing capacity R_{uP} (Dithinde *et al*. 2011). If M = 1 is assumed in the reliability analysis, the model uncertainty is not considered, which means that R_{uP} is considered as the real value of the ultimate bearing capacity (R_{uR}).

2.4 Reliability analysis method

Some commonly used reliability analysis methods are the first-order reliability analysis method (FORM), the Monte Carlo simulation (MCS), and the response surface method (RSM) (Rackwitz and Fiessler 1978, Yang and Li 2017, Saseendran and Dodagoudar 2020). Among them, the FORM computes the reliability index by linearly expanding the limit state function at the design point. Although the FORM is an approximate reliability analysis method, this method considers the probability distribution types of basic variables and calculates the reliability index with acceptable accuracy and efficiency. Therefore, the FORM is widely used for the reliability analysis of geo-structures. The MCS adopts random simulations and statistical tests to compute the failure probability of engineering structures. The accuracy of the MCS increases with the number of simulations. If the simulations are enough, accurate estimation of the failure probability can be obtained. Thus, the MCS is often used to verify the correctness of other methods. The FORM is adopted to perform the reliability analysis of the piles in this study. The iterative formulas of the FORM are as follows

$$\beta = \frac{g(\boldsymbol{x}^*) - \sum_{i=1}^{n} \frac{\partial g(\boldsymbol{x}^*)}{\partial X_i} \cdot (x_i^* - \mu_{X_i})}{\sqrt{\sum_{i=1}^{n}\sum_{j=1}^{n} \frac{\partial g(\boldsymbol{x}^*)}{\partial X_i} \frac{\partial g(\boldsymbol{x}^*)}{\partial X_j} \rho_{X_i X_j} \sigma_{X_i} \sigma_{X_j}}} \tag{10a}$$

$$\alpha_{X_i} = -\frac{\sum_{k=1}^{n} \frac{\partial g(\boldsymbol{x}^*)}{\partial X_k} \rho_{X_i X_k} \sigma_{X_k}}{\sqrt{\sum_{i=1}^{n}\sum_{j=1}^{n} \frac{\partial g(\boldsymbol{x}^*)}{\partial X_i} \frac{\partial g(\boldsymbol{x}^*)}{\partial X_j} \rho_{X_i X_j} \sigma_{X_i} \sigma_{X_j}}} \tag{10b}$$

$$x_i^* = \mu_{X_i} + \alpha_{X_i} \beta \sigma_{X_i} \tag{10c}$$

where $\boldsymbol{X} = [X_1, \ldots, X_n]$ is the basic variable vector (n is the number of basic variables); $\boldsymbol{x}^* = [x_1^*, x_2^*, \ldots, x_n^*]$ is the design point; $g(\boldsymbol{x}^*)$ is the function value at the design point; $\partial g(\boldsymbol{x}^*) / \partial X_i$ is the derivative of the limit state function with respect to basic variable X_i; ρ_{XiXj} is the correlation coefficient between variables X_i and X_j; μ_{Xi} and σ_{Xi} are the mean and standard deviation of variable X_i, respectively; α_{Xi} is the directional cosine; and β is the reliability index.

Eq. (10) is only suitable for the cases that all the basic variables are normally distributed. If basic variable X_i is non-normally distributed, it should be first converted to an equivalent normal variable X_i', and then use μ_{Xi}' and σ_{Xi}' to replace μ_{Xi} and σ_{Xi} in Eq. (10) for the iterative computation of reliability index.

3. Statistical analyses of static load test data

3.1 Database description

A large amount of vertical compressive Q-s data was collected in Anhui province, China. Among them, there are 42 sets of the destructive Q-s data collected from 10 sites and 635 sets of the proof Q-s data collected from 14 sites. The pile type, the number of piles in each site, the pile diameter and length, the pile spacing, the group piles' layout, and the types of soil along the pile are shown in Tables 1 and 2 for the destructive and proof tests, respectively. In Table 2, The N_1 column represents the number of piles collected from each site, and the N_2 column represents the number of piles after deleting the piles whose Q-s curves are abnormal. In Tables 1 and 2, CBP, PHC, and CFG represent cast-in-suit bored piles, prestressed high-strength concrete pipe piles, and cement fly-ash gravel piles, respectively.

Table 2 Information of proof static load tests

Site	Pile types	Number of piles		Pile diameter (m)	Pile length (m)	Pile spacing (m)	Group piles' layout	Types of soil along the piles
		N_1	N_2					
P1	PHC	57	48	0.6	14	2.4	Square	Clay and weathered sandstone
P2	PHC	65	57	0.4	13	1.4	Double piles	Clay and weathered sandstone
P3	CFG	68	54	0.4	14	1.6	Square	Clay
P4	PHC	35	30	0.5	42	1.8	Double piles and square	Silty clay and silty sand
P5	CBP	35	30	0.6	17	1.8	Square and triangle	Silty clay and silty sand
P6	CBP	67	48	0.8	10	8.0	Square	Silty clay, coarse sand and weathered sandstone
P7	PHC	15	15	0.5	14	1.9	Square and triangle	Silty clay and clay
P8	PHC	57	57	0.5	14	1.9	Square and triangle	Silty clay and clay
P9	CFG	22	9	0.4	21	2.0	Square	Silt, silty clay and silty sand
P10	CBP	21	19	0.4	26	2.9	Double piles	Silty clay and weathered siltstone
P11	CBP	21	21	0.6	26	1.8	Three piles in one line	Silty clay and weathered siltstone
P12	PHC	15	11	0.5	30	2.0	Square	Clay, silty clay and silt
P13	CFG	41	40	0.4	15	1.7	Square	Silty clay and silt
P14	CFG	28	19	0.5	13	1.7	Square	Silty clay and clay

Table 3 Statistics of fitting parameters a, b and the limit settlement s_a

Site	Parameter a			Parameter b			Parameter s_a			Correlation coefficient		
	μ_a ($\times10^{-3}$) (mm/kN)	δ_a	Prob. dist.	μ_b ($\times10^{-4}$) (1/kN)	δ_b	Prob. dist.	μ_{sa} (mm)	δ_{sa}	Prob. dist.	$\rho_{a\text{-}b}$	$\rho_{a\text{-}sa}$	$\rho_{b\text{-}sa}$
P1	2.10	0.22	LN	1.88	0.22	N	15.76	0.13	LN	-0.84	0.93	-0.97
P2	1.60	0.36	LN	1.78	0.24	N	12.89	0.18	LN	-0.71	0.94	-0.88
P3	5.24	0.28	LN	3.81	0.22	N	14.52	0.14	LN	-0.27	0.81	-0.75
P4	1.01	0.34	LN	0.70	0.35	LN	16.32	0.26	LN	-0.54	0.82	-0.78
P5	0.76	0.34	LN	0.44	0.59	LN	20.42	0.40	LN	-0.46	0.51	-0.76
P6	0.55	0.24	N	0.78	0.42	LN	17.39	0.51	LN	-0.23	0.24	-0.59
P7	2.10	0.24	LN	1.25	0.17	LN	16.75	0.15	LN	-0.85	0.97	-0.94
P8	3.00	0.21	LN	1.84	0.16	LN	16.36	0.12	LN	-0.80	0.96	-0.93
P9	1.94	0.33	LN	0.51	0.77	LN	24.63	0.34	LN	0.63	-0.26	-0.81
P10	1.00	0.31	LN	2.02	0.10	LN	12.57	0.08	LN	-0.40	0.97	-0.60
P11	1.80	0.28	LN	3.08	0.13	LN	13.05	0.10	LN	-0.86	0.98	-0.93
P12	1.20	0.33	LN	1.00	0.44	LN	15.38	0.19	LN	-0.82	0.90	-0.96
P13	5.00	0.39	N	4.21	0.30	LN	14.09	0.22	LN	-0.89	0.97	-0.95
P14	2.41	0.46	LN	1.71	0.50	LN	17.94	0.49	LN	-0.25	0.63	-0.74

Note: N and LN represent normal and lognormal distribution, respectively

3.2 Statistical analysis of model factor M

3.2.1 Computation of model factor M

According to the definition of the model factor in Eq. (4), the model factor M is estimated based on the destructive Q-s data as follows:

Step 1: Compute the predicted value of the ultimate bearing capacity (R_{uP}): Select the predetermined load for the proof test according to the test report of the site and consider those points whose load are less than the predetermined load as the proof Q-s data. Then, fit the curve with these proof Q-s data and the hyperbolic model (Eq. (1)) to obtain the Q-s curve and estimate R_{uP} based on the Q-s curve using the slope tangent method.

Step 2: Compute the real value of the ultimate bearing capacity (R_{uR}): Similarly, fit the curve using all destructive Q-s data, and estimate R_{uR} based on this Q-s curve according to the slope tangent method.

Step 3: Calculate the model factor M according to Eq. (4).

Repeat the above steps for all the 42 sets of destructive Q-s data.

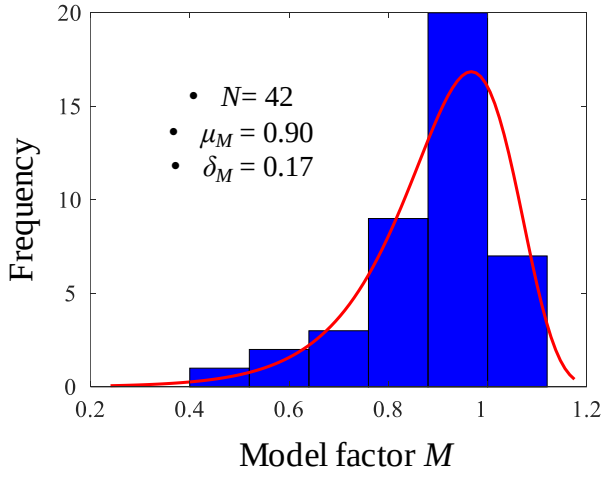

Fig. 3 Statistics of model factor M

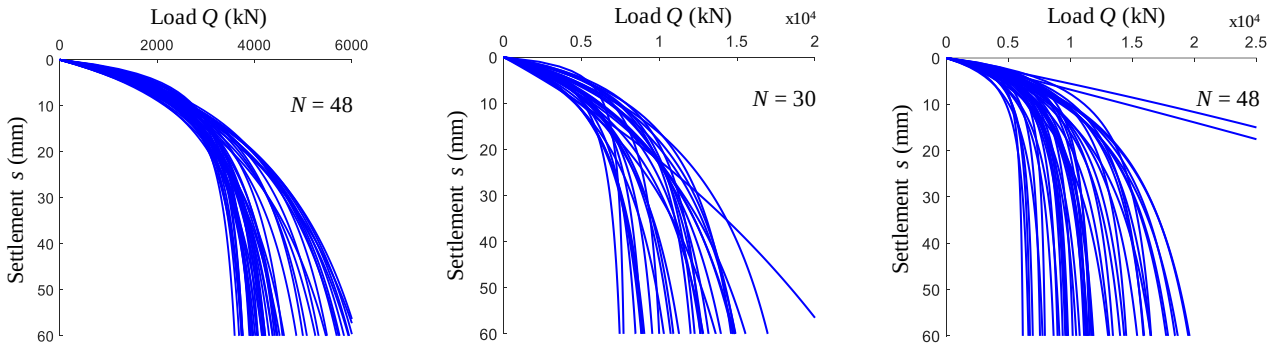

(a) Site P1 (b) Site P4 (c) Site P6

Fig. 4 Q-s curves of proof static load tests

3.2.2 Statistical model factor M

As shown in Table 1, there are only 3 to 6 sets of the destructive Q-s data in each site. Consequently, only 3 to 6 model factors are obtained in each site. The accuracy of the statistics characteristics of model factors of each site estimated by such small amount of data is doubtful. Therefore, all the 42 sets of destructive Q-s data described in Table 1 were put together to investigate the statistics characteristics of M. To some extent, this can be categorized as the Level C Design due to the limitation of the insufficient data (Roberts 2010). Moreover, many authors had conducted relevant studies according to Q-s data collected from different locations (Chen *et al*. 2008, 2014, Uzielli and Mayne 2012, Phoon and Ching 2017, Asem and Gardoni 2019). For example, Chen et al. (2008) used 77 sets of the drained and undrained data from 33 different references to establish a consistent uplift interpretation criterion to evaluate the capacity of drilled shaft foundations under axial uplift loading. Phoon and Ching (2017) statistically analyzed the load test data of 47 sets of piles from 29 countries with different pile types, pile dimensions, and soil layer distributions. Uzielli and Mayne (2012) investigated the statistics of Q-s fitting parameters based on 30 sets of shallow foundation Q-s data from different countries. Asem and Gardoni (2019) used the limited load test data to develop an empirical framework for the prediction of the load-transfer function for side resistance of sockets.

The frequency distribution histogram of model factors and the corresponding fitted frequency distribution curve are plotted in Fig. 3. As shown in Fig. 3, the optimal probabilistic distribution of M is Gumbel distribution, which is proved by the Kolmogorov-Smirnov test (Marsaglia *et al*. 2003). The mean and coefficient of variation (COV) of M are $\mu_M = 0.90$ and $\delta_M = 0.17$, respectively. Although the destructive Q-s data were collected from different construction sites and the typesand sizes of the piles were different, the COV of M is relevantly small compared to the COVs of geotechnical parameters in references (Phoon and Tang 2019). Accordingly, the statistics of M shown in Fig. 3 are used in the next section for the reliability analysis of piles.

3.3 Statistical analyses of parameters a, b and s_a

3.3.1 Judgement of abnormal Q-s curves

Before performing statistical analyses for Q-s fitting parameters, abnormality of the Q-s curves should be identified and deleted. Trial calculation shows that here are mainly two types of abnormal Q-s curves.

Type1: The fitting parameters a or b is negative. When the fitting parameters a or b is negative, the trend of the Q-s fitting curve is opposite to the normal Q-s curve. The abnormal Q-s curve is concave in the Q-s coordinate system, while the normal Q-s curve is convex in the same coordinate system.

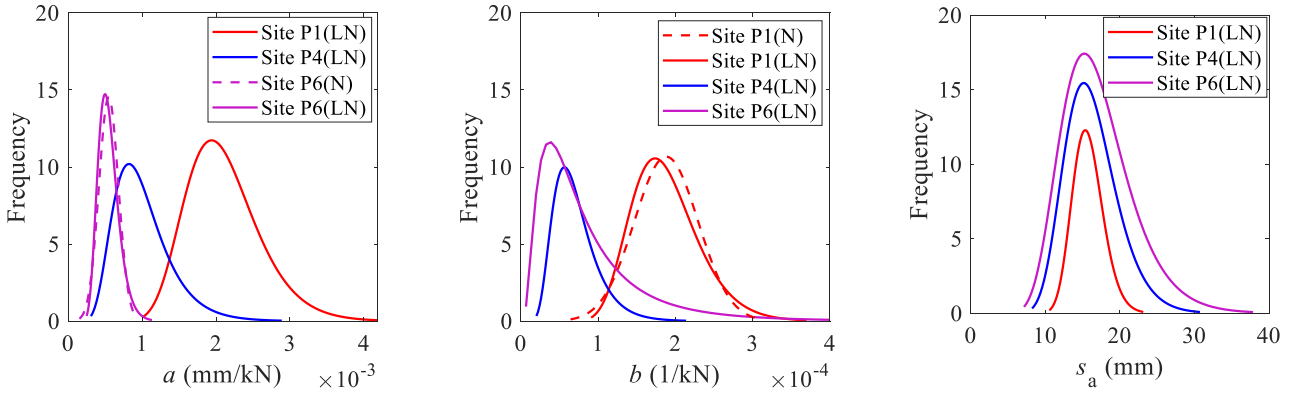

(a) Fitting parameter a (b) Fitting parameter b (c) Limit settlement s_a

Fig. 5 Probabilistic distributions of parameters a, b, and s_a

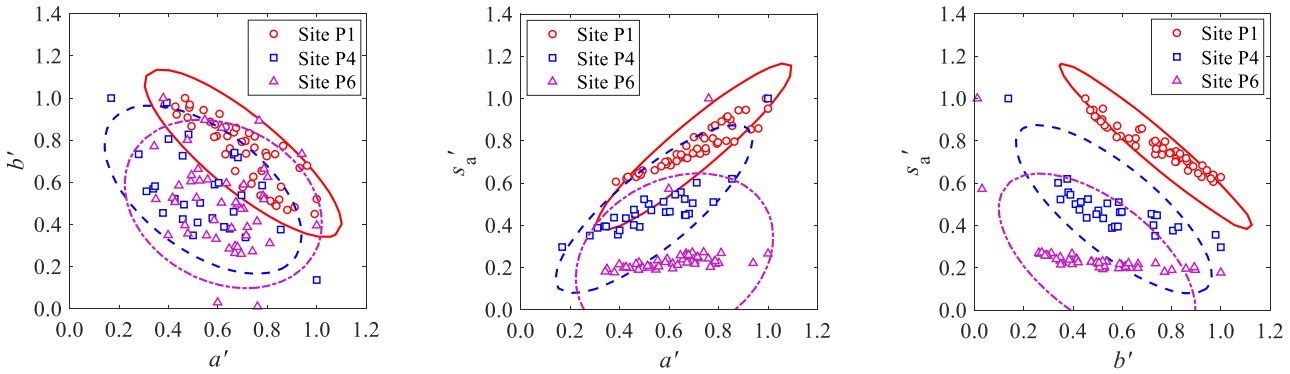

(a) Correlation between a' and b' (b) Correlation between a' and s_a' (c) Correlation between b' and s_a'

Fig. 6 Correlations among parameters a, b, and s_a

Therefore, the Q-s curves whose fitting parameter a or b are negative should be deleted.

Type2: The location of this type of curve is far away from other Q-s curves of piles in the same engineering site. The reason of the abnormal curves is that the fitting parameters a and b are very different from the those of the other curves. Thereby, this type of abnormal Q-s curves should be deleted according to the three-sigma rule (i.e., the 3σ principle) (Duncan 2000; Phoon *et al*. 2010).

3.3.2 Statistical analysis of parameters a, b and s_a after deleting the abnormal Q-s curves

After deleting the abnormal curves, statistical analysis is performed on N_2 sets of Q-s curves for each site in Table 2. The statistics (i.e., the mean (μ), the COV (δ), the optimal probability distribution type, and the correlation coefficient (ρ)) of parameters a, b, and s_a are listed in Table 3. The corresponding Q-s curves and the optimal probabilistic distribution curves of parameters a, b, and s_a of Sites P1, P4, and P6 are shown in Figs. 4 and 5. The corresponding figures of other sites are similar to the Figs. 4 and 5 and not shown here for reason of space.

Fig. 4 demonstrates that the Q-s curves of different piles at a site fluctuate in a large range, which results in the large variability of the ultimate bearing capacities of piles. It is further observed that the variability of the ultimate bearingcapacity is reflected by the COV of parameter b (δ_b).

For example, the COVs of parameter b (δ_b) of Sites P1, P4, and P6 are 0.22, 0.35, and 0.42, respectively. Therefore, the ranges of variation of the Q-s curves of Sites P1, P4, and P6 increase gradually.

Table 3 shows that the optimal probabilistic distributions of parameters a, b, and s_a are mainly lognormal (LN). Among all optimal probabilistic distributions, only two parameters of a (Sites P6 and P14) and three parameters of b (Sites P1, P2, and P3) are normally distributed. Taking Sites P1, P4, and P6 as examples, the optimal fitted frequency distribution curves of parameters a, b, and s_a are shown in Fig. 5. For comparison, the corresponding normal frequency distribution curves of parameter a of Site P6 and parameter b of Site P1 are also plotted in Figs. 5(a) and 5(b), respectively. It is apparent that the fitted normal and lognormal frequency distribution curves of parameter a of Site P6 almost coincide in Fig. 5(a), and the fitted normal and lognormal frequency distribution curves of parameter b of Site P1 are also very close to each other in Fig. 5(b). This implies that the frequency distributions of parameters a, b, and s_a can be assumed to be lognormally distributed in the subsequent calculations.

Taking Sites P1, P4, and P6 as examples, the scatter diagram of the normalized parameters of a', b', and s_a' are shown in Fig. 6. The normalization of parameters a, b, and s_a is as follows

$$a' = a/a_{\max},\ b' = b/b_{\max},\ s_a' = s_a/s_{a\max} \tag{11}$$

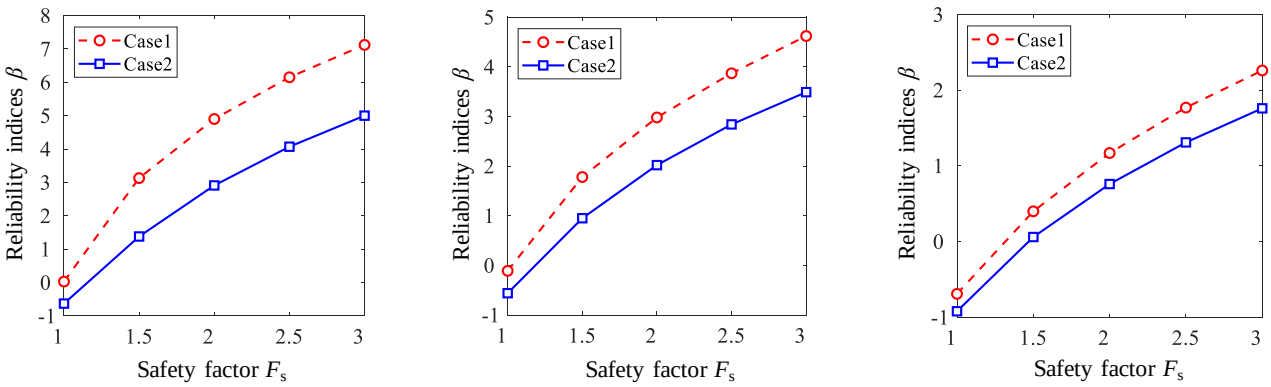

(a) Site P1 (b) Site P4 (c) Site P6

Fig.7 Comparison of reliability indices β of different variable combinations

Table 4 Reliability indices and safety judgment of piles (F_s = 2.0, β^T=3.2)

Site	Case 1		Case 2	
	$\beta_{1\text{-FORM}}$	$\beta_1 \geq \beta^T$?	$\beta_{2\text{-FORM}}$	$\beta_2 \geq \beta^T$?
P1	4.90	Yes	2.91	No
P2	4.47	Yes	2.78	No
P3	4.33	Yes	2.52	No
P4	2.98	No	2.02	No
P5	1.43	No	1.03	No
P6	1.17	No	0.76	No
P7	7.12	Yes	3.60	Yes
P8	7.76	Yes	3.63	Yes
P9	0.93	No	0.68	No
P10	6.99	Yes	3.50	Yes
P11	7.93	Yes	3.75	Yes
P12	2.57	No	1.90	No
P13	4.04	Yes	2.73	No
P14	1.30	No	0.90	No

where a', b', and s_a' are the normalized parameters of a, b, and s_a, respectively; a_{max}, b_{max}, and s_{amax} are the maximum values of parameters a, b, and s_a in a site, respectively. The purpose of the normalization of parameters a, b, and s_a is to remove the influence of variable units so that different parameters can be plotted in the same graph.

Fig. 6 shows that the scatters of (a', b'), (a', s_a'), and (b', s_a') of each site are almost concentrated in an ellipse. The angle between the major axis of an ellipse and the positive direction of the x-axis in Fig. 6 indicates the sign of the correlation between the two parameters in each sub-figure. When the angle lies in [0, 90°], the two parameters in each sub-figure are positively related to each other; on the contrary, when the angle lies in [90°, 180°], the two parameters in each sub-figure are negatively related to each other. The length of the minor axis of an ellipse indicates the magnitude of the correlation between two parameters. A small minor axis of an ellipse implies that the scatters are more likely to be centered along the major axis of the ellipse, which corresponds to a relatively great correlation between the two parameters in each sub-figure. For the three sites shown in Fig. 6, parameters a and s_a are positively correlated, whereas parameters a and b, and b and s_a are both negatively correlated. These conclusions are almost consistent with all values listed in the three rightmost columns in Table 3 except for Site P9.

4. Reliability calculations

After obtaining the statistical information of model factors M (Fig. 3) and parameters a, b, and s_a (Table 3), the reliability analyses of each site listed in Table 2 can be performed using the FORM based on the ultimate limit state function (Eq. (9)). The focus of this paper is to analyze the influence of the uncertainty of the ultimate bearing capacity of piles. For simplify, the load Q is deemed as a deterministic value which be estimated by Eq. (6). To investigate the influence of M on the reliability of piles, two cases of basic variables are considered. Case1: Assume the basic variables to be $\boldsymbol{X} = [a, b, s_a]$ and $M = 1$. This assumption implies that the model uncertainty for the prediction of ultimate bearing capacity is ignored. Case2: Consider the influence of M on the reliability of piles. Thus, the basic variable is $\boldsymbol{X} = [a, b, s_a, M]$. Taking Sites P1, P4 and P6 as examples, the relationship between the

reliability index β and the safety factor F_s under the two calculation conditions are shown in Fig. 7. The reliability indices without considering the model uncertainty (Case 1) are always larger than those with the consideration of model uncertainty (Case 2). Therefore, carrying out the reliability analysis based on the proof *Q-s* data will overestimate the reliability of piles, which will result in dangerous assessment and design.

In the traditional and probabilistic design specifications of piles (Kim and Salgado 2012), the allowable safety factor (F_s) is recommended to be 2.0 and the target reliability index (β^T) is recommended to be 3.2. Under the assumption of F_s = 2.0 and β^T=3.2, the reliability indices of all sites with proof *Q-s* data are summarized in Table 4. It demonstrates that among the 14 sites with proof *Q-s* data, four sites meet the requirement of $\beta \geq \beta^T$ for Case 2, while eight sites meet the requirement of $\beta \geq \beta^T$ for Case 1. This proves again that ignoring the model uncertainty of ultimate bearing capacity will lead to dangerous assessment of piles.

5. Conclusions

A reliability analysis method based on the proof *Q-s* data of plies under vertical load is proposed. By defining the real ultimate bearing capacity (R_{uR}) as the product of the model factor (M) and the predicted ultimate bearing capacity (R_{uP}), the reliability analyses of piles in different construction sites can be easily performed based on the statistics characteristics of model factors and the large amount of proof *Q-s* data in different construction sites. The main conclusions are as follows:

- A method for estimating the model factor (M) of ultimate bearing capacity is proposed based on the comparison between the destructive and the proof *Q-s* data. The statistical characteristics of the model factors of different sites are obtained based the destructive *Q-s* data, where the variability of the model factors is not significant under different geological conditions.
- A simple ultimate limit state function is derived for the reliability analysis according to the hyperbolic fitting model of the *Q-s* curve and the relationship between the model factor (M) and the real ultimate bearing capacity (R_{uR}). The statistics characteristics of the three variables (a, b, and s_a) are easily estimated by fitting the proof *Q-s* data and the slope tangent method.
- The influence of model uncertainty of the ultimate limit state function on the reliability of piles is investigated. Ignoring model uncertainty results in the reliability index is bigger than that considering model uncertainty. This indicates that model uncertainty is an important basic variable in the reliability analysis, and ignoring model uncertainty will lead to dangerous assessments and designs.

Note that the number of destructive *Q-s* data of each site is very limited due to the high cost of destructive static load test, it cannot assure the accuracy of the statistics characteristics of model factor of each sites. Therefore, the statistics characteristics of model factor are estimated by the destructive *Q-s* data from different construction sites in this study. The accuracy of the statistics characteristics of model factors computed from different sites might be improved by Bayesian updating based on the experimental data of a specific site, which is the focus of our future study.

Acknowledgments

This work was supported by the National Natural Science Foundation, China (41972278).

References

Asem, P. and Gardoni, P. (2019), "A load-transfer function for the side resistance of drilled shafts in soft rock", *Soils Found.*, **59**, 1241-1259. https://doi.org/10.1016/j.sandf.2019.04.006.

Chen, Y.J., Chang, H.W. and Kulhawy, F.H. (2008), "Evaluation of uplift interpretation criteria for drilled shaft capacity", *J. Geotech. Geoenviron. Eng.*, **134**, 1459-1468. https://doi.org/10.1061/(ASCE)1090-0241(2008)134:10(1459).

Chen, Y.J., Liao, M.R., Lin, S.S., Huang, J.K. and Marcos, M.C.M. (2014), "Development of an integrated Web-based system with a pile load test database and pre-analyzed data", *Geomech. Eng.*, **7**(1), 37-53. https://doi.org/10.12989/gae.2014.7.1.037.

Chinese Standard (2014), "Technical Code for Testing of Building Foundation Piles", JGJ106-2014. (in Chinese)

Ching, J.Y. and Chen, J.R. (2010), "Predicting displacement of augered cast-in-place piles based on load test database", *Struct. Saf.*, **32**(6), 372-383. https://doi.org/10.1016/j.strusafe.2010.04.007.

Davisson, M.T. (1972), "High Capacity Piles", Proceedings of the Soil Mechanics Lecture Series on Innovations in Foundation Construction, New York: American Society of Civil Engineers.

Dithinde, M., Phoon, K.K., De, W.M. and Retief, J.V. (2011), "Characterization of model uncertainty in the static pile design Formula", *J. Geotech. Geoenviron. Eng.*, **137**(1), 70-85. https://doi.org/10.1061/(ASCE)GT.1943-5606.0000401.

Duncan, J.M. (2000), "Factors of Safety and Reliability in Geotechnical Engineering", *J. Geotech. Geoenviron. Eng.*, **126**(4), 307-316. https://doi.org/10.1061/(ASCE)1090-0241(2000)126:4(307).

Fei, S.Z., Tan, X.H., Gong, W.P., Dong, X.L., Zha, F.S. and Xu, L. (2021), "Reliability analysis of strip footing under rainfall using KL-FORM", *Geomech. Eng.*, **24**(2), 167-178. https://doi.org/10.12989/gae.2021.24.2.167.

Hirany, A. and Kulhawy, F.H. (2002), "On the Interpretation of Drilled Foundation Load Test Results", in: Deep Foundations 2002. American Society of Civil Engineers, Orlando, Florida, United States, 1018-1028. https://doi.org/10.1061/40601(256)71.

Huffman, J.C., Strahler, A.W. and Stuedlein, A.W. (2015), "Reliability-based serviceability limit state design for immediate settlement of spread footings on clay", *Soils Found.*, **55**(4), 798-812. https://doi.org/10.1016/j.sandf.2015.06.012.

Jia, L., Guo, J. and Yao, K. (2018), "In situ monitoring of the long-term settlement of high-fill subgrade", *Adv. Civil Eng.*, 2018, 1347547. https://doi.org/10.1155/2018/1347547.

Khorrami, R. and Derakhshani, A. (2019), "Estimation of ultimate bearing capacity of shallow foundations resting on cohesionless soils using a new hybrid M5'-GP model", *Geomech. Eng.*, **19**(2), 127-139. https://doi.org/10.12989/gae.2019.19.2.127.

Kim, D. and Salgado, R. (2012), "Load and resistance factors for internal stability checks of mechanically stabilized earth walls", *J. Geotech. Geoenviron. Eng.*, **138**(8), 910-921. https://doi.org/10.1061/(ASCE)GT.1943-5606.0000664.

Kim, H.J. and Mission, J.L. (2011), "Probabilistic evaluation of economical factor of safety for the geotechnical design of pile

axial load capacity", *KSCE J. Civil Eng.*, **15**(7), 1167-1176. https://doi.org/10.1007/s12205-011-0948-8.

Lee, J., Kim, M. and Lee, S.H. (2009), "Reliability analysis and evaluation of LRFD resistance factors for CPT-based design of driven piles", *Geomech. Eng.*, **1**(1), 17–34. https://doi.org/10.12989/gae.2009.1.1.017.

Luo, Z.Y., Dong, Q.H. and Gong, X.N. (2004), "Application of gray system theory to determining ultimate bearing capacity of a single pile", *Rock Soil Mech.*, 2, 304-307. (in Chinese)

Marsaglia, G., Tsang, W.W. and Wang, J.B. (2003), "Evaluating Kolmogorov's distribution", *J. Stat. Software*, 008(i18). https://doi.org/10.18637/jss.v008.i18.

Misra, A. and Roberts, L.A. (2009), "Service limit state resistance factors for drilled shafts", *Geotechnique*, **59**(1), 53-61. https://doi.org/ 10.1680/geot.2008.3605.

O'Neil, M.W. and Reese, L.C. (1990), "Drilled shafts: Construction procedures and design methods", *Tunn. Undergr. Sp. Tech.*, **5**(1), 156-157. https://doi.org/10.1016/0886-7798(90)90101-O.

O'Rourke, T.D. and Kulhawy, F.H. (1985), "Observations on load tests on drilled shafts", in: Drilled Piers & Caissons II. New York.

Phoon, K.K. and Ching, J.Y. (2017), "Risk and Reliability in Geotechnical Engineering", CRC Press, Boca Raton. https://doi.org/10.1201/b17970.

Phoon, K.K., Santoso, A. and Quek, S.T. (2010), "Probabilistic analysis of soil-water characteristic curves", *J. Geotech. Geoenviron. Eng.*, **136**(3), 445-455. https://doi.org/10.1061/(ASCE)GT.1943-5606.0000222.

Phoon, K.K. and Tang, C. (2019), "Effect of extrapolation on interpreted capacity and model statistics of steel H-piles", *Georisk-Assessment and Management of Risk for Engineered Systems and Geohazards*, **13**(4), 291–302. https://doi.org/10.1080/17499518.2019.1652920.

Rackwitz, R. and Fiessler, B. (1978), "Structural reliability under combined random load sequences", *Comput. Struct.*, **9**(5), 489-94. https://doi.org/10.1016/0045-7949(78)90046-9.

Roberts, L.A. (2010), "Performance-Based Design of Deep Foundation Systems in Load and Resistance", *Transportation Research Record*, 2186, 29-37. https://doi.org/10.3141/2186-04.

Saseendran, R. and Dodagoudar, G.R. (2020), "Reliability analysis of slopes stabilised with piles using response surface method", *Geomech. Eng.*, **21**(6), 513-525. https://doi.org/10.12989/gae.2020.21.6.513.

Selig, E. and ISSMFE. (1985), "Axial pile loading test—Part 1: Static loading", *Geotech. Test. J.*, **8**(2), 79. https://doi.org/10.1520/GTJ10514J.

Tan, X.H., Xie, Y., Hou, X.L., Li, P. and Wang, X. (2017), "Reliability Analysis of Shallow Foundations on Unsaturated Soils under Rainfall Infiltration", *Geo-Risk 2017: Geotechnical Risk Assessment and Management*, 588–597.

Uzielli, M. and Mayne, P.W. (2012), "Load-displacement uncertainty of vertically loaded shallow footings on sands and effects on probabilistic settlement estimation", *Georisk*, **6**(1), 50–69. https://doi.org/10.1080/17499518.2011.626333.

Yang, X.L. and Li, W.T. (2017), "Reliability analysis of shallow tunnel with surface settlement", *Geomech. Eng.*, **12**(2), 313-326. https://doi.org/10.12989/gae.2017.12.2.313.

Zhang, Q.Q., Liu, S.W., Zhang, S.M., Zhang, J. and Wang, K. (2016), "Simplified non-linear approaches for response of a single pile and pile groups considering progressive deformation of pile–soil system", *Soils Found.*, **56**(3), 473-484. https://doi.org/10.1007/s11771-013-1072-9.